AIMS Mathematics, 9(5): 12726–12750.
DOI: 10.3934/math.2024622
Received: 20 January 2024
Revised: 23 February 2024
Accepted: 28 February 2024
Published: 02 April 2024

http://www.aimspress.com/journal/Math

Research article

Extraction of PEM fuel cell parameters using Walrus Optimizer

Essam H. Houssein[1], Nagwan Abdel Samee[2], Maali Alabdulhafith[2,*] and Mokhtar Said[3]

[1] Faculty of Computers and Information, Minia University, Minia 61519, Egypt
[2] Department of Information Technology, College of Computer and Information Sciences, Princess Nourah bint Abdulrahman University, P.O. Box 84428, Riyadh 11671, Saudi Arabia
[3] Electrical Engineering Department, Faculty of Engineering, Fayoum University, Fayoum 43518, Egypt

* **Correspondence:** Email: MIAlabdulhafith@pnu.edu.sa.

Abstract: The process of identifying the optimal unknown variables for the creation of a precision fuel-cell performance forecasting model using optimization techniques is known as parameter identification of the proton exchange membrane fuel cell (PEMFC). Recognizing these factors is crucial for accurately forecasting and assessing the fuel cell's performance, as they may not always be included in the manufacturer's datasheet. Six optimization algorithms—the Walrus Optimizer (WO), the Tunicate Swarm Algorithm (TSA), the Harris Hawks Optimizer (HHO), the Heap Based Optimizer (HBO), the Chimp Optimization Algorithm (ChOA), and the Osprey Optimization Algorithm (OOA) were used to compute six unknown variables of a PEMFC. Also, the proposed WO method was compared with other published works' methods such as the Equilibrium Optimizer (EO), Manta Rays Foraging Optimizer (MRFO), Neural Network Algorithm (NNA), Artificial Ecosystem Optimizer (AEO), Slap Swarm Optimizer (SSO), and Vortex Search Approach with Differential Evolution (VSDE). Minimizing the sum squares error (SSE) between the estimated and measured cell voltages requires treating these six parameters as choice variables during optimization. The WO algorithm yielded an SSE of 1.945415603, followed by HBO, HHO, TSA, ChOA, and OOA. Given that WO accurately forecasted the fuel cell's performance, it is appropriate for the development of digital twins for fuel cell applications and control systems for the automobile industry. Furthermore, it was shown that the WO convergence speed was faster than the other approaches studied.

Keywords: Walrus optimizer; fuel cell; parameter extraction; proton exchange membrane fuel cell
Mathematics Subject Classification: 68TXX

1. Introduction

Sustainable energy sources are becoming more and more crucial for both small-scale power applications and big industrial uses due to the rapid depletion of fossil fuel supplies and the growing demand for electricity. Metaheuristic algorithms are applied to solve in several applications [1–11]. Renewable energy sources, such as wind and solar power, are frequently reliant on their surroundings. Fuel cells were developed as a result to complement the available green energy sources. Fuel cells have historically been divided into three categories: transportation-related, stationary, and portable [12]. The growing usage of fuel cells for large land vehicles, such as public buses, has led to a rapid advancement in the automotive fuel cell technology field. Furthermore, stationary fuel cells for use in homes and workplaces are becoming more common [13]. Stationary fuel cells have various applications. In recent years, many businesses and researchers have been interest in fuel cells. The chemical energy produced by the reaction of oxygen and hydrogen, or ambient air, can be quickly converted into electrical energy using fuel cells [14]. Phosphoric acid, solid oxide, alkaline, and proton exchange membrane fuel cells are only a few of the many types of fuel cells [15]. PEMFC fuel cells are the most often used fuel cell type in the automotive sector, despite the fact that each of these fuel cell types has a distinct purpose [16,17].

Currently, there are a number of well-established concepts in the literature that can be utilized to determine the exact PEMFC parameters. Most of these optimization-based methods are considered to be simple, dependable, and uniform [18]. The optimal PEMFC parameters have been the subject of numerous studies that have been published in the literature. For instance, a study was carried out to ascertain the parameters of a circuit that is comparable to a PEMFC utilizing a multiverse optimizer [19]. For the investigation, a total of seven criteria were taken into account. Numerous optimization parameters that ensure convergence were found in reports similar to this one from other authors [20]. With an emphasis on evolutionary techniques, swarm physics, and nature, the numerous approaches were neatly categorized. Furthermore, several metaheuristics for microgrid optimization were evaluated by Hegazy et al. [21]. In an attempt to reduce the sum squared error (SSE), adaptive sparrow search strategies were also explored to evaluate the discrepancy between the measured and computed voltage [22]. Yousri et al. [23] determined that the fractional-order modified Harris hawk optimizer was the best algorithm for mathematical modeling of PEMFCs. Other authors were able to further reduce the discrepancy between the estimated and empirical values by using a novel optimization strategy that they developed [20]. Experiment in [24] made use of two distinct types of fuel cells. Using an enhanced monarch butterfly optimizer has also been looked into as a way to ensure a reduction in the integral time absolute error [25]. The enhanced Chimp Optimizer was also used to test three commercial fuel cells. The study used a 15-nature strategy to confirm its conclusions. The artificial ecosystem-based algorithm beat the grey wolf, particle swarm, slime mold, and Harris hawk optimizers in terms of outcomes, according to Tabbi et al. [26].

The literature has also proposed a hybrid method that combines a vortex search algorithm and differential evolution to find the optimal parameters for PEMFCs [27]. According to theoretical inferences made from the experimental findings, the SSE was considered to be the best fitness function between the voltages created for the stack. Additionally, a monarch butterfly optimizer was tested in a range of settings using a 250 W PEMFC stack [28]. Using a sunflower optimizer, Yuan et al. [29] calculated the unknown parameters for PEMFCs. A converged moth search technique has also been reported in the literature to be effective in reducing the SSE between the measured and experimental

voltages [30]. Syah et al. [31] used a balanced strider approach to reduce the total squared difference between the experimental and numerical voltages. The goal was also to determine the cost of the stack using a modified grass fibrous root technique [32]. Mossa et al. [33] mainly used the Atom Search Algorithm and the Harris Hawk optimizers to estimate the unknown values for PEMFCs. The SSE value for the measured and mathematical data was used to calculate the fitness function. Rezk et al. [34] used a gradient-based strategy and compared it with alternative ways to find the ideal parameters between three distinct types of fuel cells. A chaos owl search optimizer has also been utilized to reduce the sum squared deviation for both measured and mathematically generated voltages [35]. A chaotic binary shark scent optimizer was also used to estimate the unknown data for a PEMFC [36]. Additionally, the unknown parameters of the fuel cell were found using a heterogeneous, comprehensive learning Archimedes optimizer [37].

Additionally, it has been reported that SSE is the goal of a semi-empirical model for PEMFCs [38]. Lu et al. [39] used the crow search approach to determine unknown parameters by reducing the integral absolute error across the various voltage types. Similar to this, fuel cell unknown values have been estimated using an equilibrium optimizer [40]. The best parameters for polarization curve creation can be estimated using a satin bowerbird method, per published research [41]. The L-SHADE-EpSin technique was used in the literature to construct a model for PEMFC estimation [42]. Isa et al. [43] investigated the use of an antlion algorithm and a dragonfly algorithm to predict unknown parameters for PEMFCs. Song et al. utilized Harris Hawk algorithms in their study on detecting fuel PEMFC parameters [44]. A barnacles mating optimizer was also used to study an accurate fuel-cell behavior model [45]. An Archimedes optimizer was also used in the literature, mostly to reduce the disparity between the data derived from the experimental and mathematical models [46]. It was also mentioned that an efficient way to estimate the unknown parameters for PEMFCs would be to employ a transient search optimizer [47].

The work's main objective and contribution can be summed up as follows:

- The Walrus Optimizer (WO) method, a recent metaheuristic technique, is being evaluated for its performance in resolving PEMFC issues.
- Using the suggested WO method, the six PEMFC parameters are estimated.
- The proposed WO algorithm is compared with the Osprey Optimization Algorithm (OOA), the Harris Hawks Optimizer (HHO), the Heap Based Optimizer (HBO), the Chimp Optimization Algorithm (ChOA), and the Tunicate Swarm Algorithm (TSA).
- The fitness function applied in the identification problem is the sum of square error.
- Ned Stack PS6, an actual PEM fuel cell model, is used to confirm that all comparator methods including the recommended WO method work as expected.
- Based on the convergence and robustness statistics, all algorithms are evaluated over the course of thirty separate runs.
- Also, the proposed WO method is compared with methods in others, published works, such as the Equilibrium Optimizer (EO), Manta Rays Foraging Optimizer (MRFO), Neural Network Algorithm (NNA), Artificial Ecosystem Optimizer (AEO), Slap Swarm Optimizer (SSO), and Vortex Search approach with Differential Evolution (VSDE).

The present work is structured in the following manner: Section 1 introduces the general background for the problem, a discussion of previous work, and contribution outlines. PEMFC modeling is covered in Section 2. The problem formulation for calculating PEMFC parameters is explained in Section 3. We examine the WO technique in Section 4. The PEMFC results will be

addressed in Section 5. Section 6 contains the work's conclusion.

2. Analysis of the PEM fuel cell

The importance of renewable energy sources is growing for both small-scale power applications and large-scale industrial uses due to the quick depletion of fossil fuel supplies and the increased demand for electricity [48]. Although renewable energy sources are widely employed, fuel cells have been developed as a means of supplementing the currently accessible green energy sources due to their susceptibility to environmental conditions. Fuel cells have historically been divided into three categories: transportable, portable, and stationary [49,50].

The polarization curve of a fuel cell running at 80 °C is displayed in Figure 1. There are three obvious main zones on the polarization curve. The terms concentration losses, ohmic losses, and activation losses are frequently used to describe these regions [51]. There is a nonlinear activation zone. The activation zone provides detailed information about the electrochemical process that is taking place inside the cell. Usually, ohmic losses are found in the membrane. The final part [52] discusses the mass concentration losses brought on by modifications to the concentration gradient inside the cell. The entire cell voltage is represented as V_{fc} in Eq (1) [51].

$$V_{fc} = E_{cell} - V_{act} - V_{ohmic} - V_{conc}. \tag{1}$$

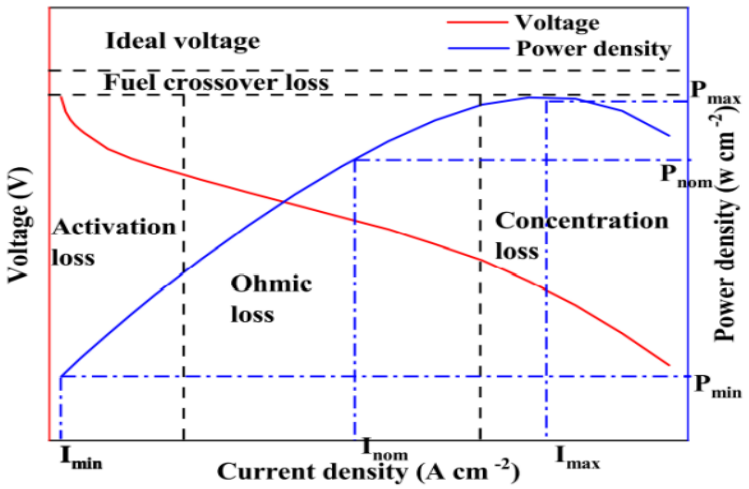

Figure 1. Losses of fuel cell.

The activation polarization is represented by V_{act}, the ohmic loss is presented by V_{ohmic}, the concentration loss is presented by V_{conc}, and the open circuit voltage is presented by E_{cell} [52]. It is also evident that the current density affects the output voltage in the ohmic part. As was already mentioned, the ionic resistance of the electrolyte also affects the slope. The concentration loss is brought on by the mass transfer limitations that cause the voltage to decrease precipitously to zero. The number of cells (X_n) connected in series determines how much the cell's total output voltage (V_t) can increase, as demonstrated by Eq (2) [48].

$$V_t = X_n - V_{cell}. \tag{2}$$

Equation (3) [48] shows how other parameters that take into consideration the variation in

temperature surrounding the cell are also taken into account. E_{cell} is essentially the open circuit voltage [53].

$$E_{cell} = \begin{cases} 1229 - \frac{44.43}{z*F}(T - 298.15) + \frac{r*T}{z*F} ln\left(P_{H2}\sqrt{P_{o2}}\right) & \forall T \leq 273 \\ 1229 - \frac{44.43}{z*F}(T - 298.15) + \frac{r*T}{z*F} ln\left(\frac{P_{H2}\sqrt{P_{o2}}}{P_{H_2O}^{Sat}}\right) & \end{cases}, \quad (3)$$

where in this work, r, F, and z stand for the ideal gas constant, the Faraday constant, and the number of moving electrons (in this case, two) respectively. The temperature of the cell is indicated by T, and the partial pressures of hydrogen (P_{H2}) and oxygen (P_{O2}) are shown. Eqs (4) and (5) provide a quantitative representation of the various partial pressure parameters [44,45].

$$P_{H2} = 0.5 \times RH_a \times P_{H_2O}^{Sat} \times \left(\left(\frac{RH_a \times P_{H_2O}^{Sat}}{P_a} \times exp\left(\frac{1.635\left(\frac{i_{cell}}{A}\right)}{T^{1.334}} \right) \right)^{-1} - 1 \right), \quad (4)$$

$$P_{o2} = RH_c \times P_{H_2O}^{Sat} \times \left(\left(\frac{RH_c \times P_{H_2O}^{Sat}}{P_c} \times exp\left(\frac{1.635\left(\frac{i_{cell}}{A}\right)}{T^{1.334}} \right) \right)^{-1} - 1 \right). \quad (5)$$

Anodic relative humidity is represented by RH_a, and cathode relative humidity is presented by RH_c. The anode pressure is P_a at the inlet and P_c at the cathode. The area of the cell is recorded as A while the current is i_{cell}. The direct relationship between temperature T and the vapor saturation parameter of water, $P_{H_2O}^{Sat}$, is expressed in Eq (6). That being said, Eq (7) is used to compute the activation losses. Eq (8) is used to compute the oxygen concentration, which is denoted by C_{o2}. The semi-empirical parametric coefficients $\delta_1, \delta_2, \delta_3, and\ \delta_4$ are employed. The ohmic losses can be computed by using Eq (9) [50].

$$log_{10}\left(P_{H_2O}^{Sat}\right) = 2.95 \times 10^{-2} \times (T - 273.15) - 9.19 \times 10^{-5} \times (T - 273.15)^2, \quad (6)$$

$$V_{act} = -\left[\delta_1 + \delta_2 T + \delta_3 T ln(C_{o2}) + \delta_4 T ln(I_{fc})\right], \quad (7)$$

$$C_{o2} = \frac{P_{o2}}{5.08 \times 10^6} exp\left(\frac{498}{T}\right), \quad (8)$$

$$V_{ohmic} = i\,(R_m + R_c). \quad (9)$$

The symbols for the electrical and ionic resistance are R_m and R_c, respectively. Eq (10) [50] is used to compute the electronic resistance, which is ascribed to the smallest variations with respect to the current and voltage, and Eq (11) is employed to ascertain the membrane parametric coefficient. Mathematical computation of the concentration polarization is done using Eq (12) [49]. The maximum current density is J_{max}, whereas J is the actual current density, and B is the parametric coefficient, also known as the diffusion parameter.

$$R_m = \rho_m \left(\frac{l}{A}\right), \tag{10}$$

$$\rho_m = \frac{181.6\left[1+0.03\left(\frac{i}{A}\right)+0.062\left(\frac{T}{303}\right)^2\left(\frac{i}{A}\right)^{2.5}\right]}{\left[\gamma-0.634-3\left(\frac{i}{A}\right)\right]\times exp\left(4.18\left(\frac{T-303}{T}\right)\right)}, \tag{11}$$

$$V_{conc} = -B \times ln\left(1 - \frac{J}{J_{max}}\right). \tag{12}$$

3. Fuel cell problem formulation of estimating PEM fuel cell parameters

It is essential to compute the six model parameters $(\delta_1, \delta_2, \delta_3, \delta_4, B, and\ \gamma)$ while developing a mathematical computational model for PEMFCs. The model parameters can be deduced from the measured data by using the SSE as an objective function for both the measured and estimated datasets.

The objective function and the variable boundaries are the two primary components of optimization algorithms. The decision variables' limitations are displayed in Table 1. The primary goal function is to minimize the sum of square error (SSE). The following formula is used to analyze SSE:

$$SSE = \sum_{i=1}^{N}\left(V_m - V_{fc}\right)^2, \tag{13}$$

where V_m is the measured voltage and N is the number of data readings.

Table 1. The limits of variables.

Parameters	Upper bound	Lower bound
δ_1	−1.19969	−0.8532
δ_2	0.0022	0.0043
δ_3	0.000034	0.000098
δ_4	−0.00026	−0.0000954
B	0	0.2
γ	23	13

4. Walrus optimizer

This section will describe the mathematical model for the Walrus Optimizer (WO) [54].

4.1. Initialization

Equation (14) illustrates how the optimization process begins with a collection of randomly generated candidate solutions (X).

$$X = LB + \text{rand}(UB - LB), \tag{14}$$

where rand is a uniform random vector in the range of 0 to 1, and LB and UB are the lower and upper limits of the problem parameters.

Agents that carry out the optimization process are called walruses. Iterations are used to continuously update their positions.

$$\mathrm{X} = \begin{bmatrix} X_{1,1}X_{1,2}\cdots X_{1,d} \\ X_{2,1}X_{2,2}\cdots X_{2,d} \\ \vdots\vdots\vdots \\ \vdots\vdots\vdots \\ X_{n,1}X_{n,2}\cdots X_{n,d} \end{bmatrix}_{n\times d}, \tag{15}$$

where d is the dimension of the design variables, and n is the population size.

All search agents' matching fitness values are kept as follows:

$$\mathrm{F} = \begin{bmatrix} (f_{1,1}f_{1,2}\cdots f_{1,d}) \\ (f_{2,1}f_{2,2}\cdots f_{2,d}) \\ \vdots\vdots\vdots \\ \vdots\vdots\vdots \\ (f_{n,1}f_{n,2}\cdots f_{nd}) \end{bmatrix}_{n\times d}. \tag{16}$$

Adult and juvenile walrus populations comprise 90% and 10% of the total population, respectively. The male to female ratio in adult walruses is 1:1.

4.2. Safety and danger signals

When it comes to roosting and foraging, walruses are extremely vigilant. One or two walruses will be on patrol as guardians, and as soon as any unforeseen circumstances are discovered, warning signals will be launched. The following is a definition of the danger and safety signals in WO:

$$Danger\ signal = A * R, \tag{17}$$

$$\alpha = 1 - t/T, \tag{18}$$

$$A = 2 \times \alpha, \tag{19}$$

$$R = 2 \times r_1 - 1. \tag{20}$$

where T is the maximum iteration, A and R are danger factors, and α declines from 1 to 0 with the number of iterations t.

The following is the definition of the safety signal in WO that corresponds to the danger signal:

$$Safety\ signal = r_2, \tag{21}$$

where r_2 and r_1 are random values that fall in the interval $(0,1)$.

4.3. Migration

Herds of walruses will move to locations better suited for population survival when danger factors become too great. The walrus position is updated in this phase as follows:

$$X_{i,j}^{t+1} = X_{i,j}^{t} + \text{migration step}, \tag{22}$$

$$migration\ step = (X_m^t - X_n^t) \cdot \beta \cdot r_3^2, \tag{23}$$

$$\beta = 1 - \frac{1}{1+\exp\left(-\frac{t-\frac{T}{2}}{T}\times 10\right)}, \tag{24}$$

where the current location of the ith walrus in the jth dimension is represented by $X_{i,j}^t$, and the new position is represented by $X_{i,j}^{t+1}$. Migration_step is the walrus movement's step size; two vigilantes are chosen at random from the population. Their positions match X_m^t and X_n^t. β is the migration step control factor, this factor varies iteratively as a smooth curve. r_3 is a random number that falls between 0 and 1.

4.4. Reproduction

When danger variables are low, walrus herds typically reproduce in currents as opposed to migrating. The lead walrus (X_{best}^t) and the male walrus (Male $_{i,j}^t$) have an influence on the female walrus during reproduction, according to the position update of female walruses. Over the course of the iteration, the female walrus becomes increasingly influenced by the leader and less by her mate.

$$\text{Female}_{i,j}^{t+1} = \text{Female}_{i,j}^t + \alpha \cdot \left(\text{Male}_{i,j}^t - \text{Female}_{i,j}^t\right) + (1-\alpha) \cdot \left(X_{\text{best}}^t - \text{Female}_{i,j}^t\right), \tag{25}$$

where $\text{Male}_{i,j}^t$ and $\text{Female}_{i,j}^t$ are the positions of the ith male and female walruses in the jth dimension, and $\text{Female}_{i,j}^{t+1}$ is the new position for the ith female walrus in the jth dimension.

Then, killer whales and polar bears frequently hunt juvenile walruses near the periphery of the population. Juvenile walruses must therefore adjust to their new position in order to evade predators.

$$\text{Juvenile}_{i,j}^{t+1} = (O - \text{Juvenile}_{i,j}^t) \cdot P, \tag{26}$$

$$\text{Juvenile}_{i,j}^{t+1} = (O - \text{Juvenile}_{i,j}^t) \cdot P, \tag{27}$$

where P is the juvenile walrus's distress coefficient, which is a random number between 0 and 1, O is the reference safety position, LF is a vector of random values that represent Lévy movement based on a Lévy distribution, and $\text{Juvenile}_{i,j}^{t+1}$ is the new position for the ith juvenile walrus in the jth dimension.

$$\text{Levy}\ (a) = 0.05 \times \frac{x}{|y|^{\frac{1}{a}}}, \tag{28}$$

where y and x are two normally distributed parameters, $x\ \text{N}(0, \sigma_x^2), y\ \text{N}(0,\ \sigma_y^2)$.

$$\sigma_x = \left[\frac{\Gamma(1+\alpha)\sin\left(\frac{\pi\alpha}{2}\right)}{\Gamma\left(\frac{1+\alpha}{2}\right)\alpha 2^{\frac{(\alpha-1)}{2}}}\right]^{\frac{1}{\alpha}}, \sigma_y = 1, \alpha = 1.5, \tag{29}$$

where σ_y and σ_x are the standard deviations, $\Gamma(x) = (x+1)!$.

Natural predators also target walruses during their underwater feeding behavior, and the animals will depart their current activity area in response to warnings from their fellows of impending danger. This behavior is seen in the late WO iteration, and walruses' ability to explore the world is aided by a certain amount of population disturbance.

$$\sigma_x = \left[\frac{\Gamma(1+\alpha)\sin\left(\frac{\pi\alpha}{2}\right)}{\Gamma\left(\frac{1+\alpha}{2}\right)\alpha 2^{\frac{(\alpha-1)}{2}}}\right]^{\frac{1}{\alpha}}, \sigma_y = 1, \alpha = 1.5, \tag{30}$$

where the distance between the best and current walrus is shown by $\left|X_{best}^{t} - X_{i,j}^{t}\right|$, and r_4 is a random value that falls between 0 and 1.

Additionally, as part of their social gathering behavior, walruses can work together to forage and migrate based on the whereabouts of other walruses in the group. By exchanging location data, walruses can assist the entire herd in locating areas of the sea where there is a greater amount of food.

$$X_{i,j}^{t+1} = (X_1 + X_2)/2, \tag{31}$$

$$\begin{cases} X_1 = X_{\text{best}}^{t} - a_1 \times b_1 \times \left|X_{\text{best}}^{t} - X_{i,j}^{t}\right| \\ X_2 = X_{\text{second}}^{t} - a_2 \times b_2 \times \left|X_{\text{second}}^{t} - X_{i,j}^{t}\right| \end{cases}, \tag{32}$$

$$a = \beta \times r_5 - \beta, \tag{33}$$

$$a = \beta \times r_5 - \beta, \tag{34}$$

$$b = \tan(\theta), \tag{35}$$

where X_{second}^{t} represents the position of the second walrus in the current iteration, $\left|X_{\text{second}}^{t} - X_{i,j}^{t}\right|$ indicates the distance between the current walrus and the second walrus, a and b are the gathering coefficients, and X_1 and X_2 are two weights influencing the walrus's gathering behavior. The random number r_5 is between 0 and 1, while the values of θ span from 0 to π.

4.5. WO code

When it comes to roosting and foraging, walruses are extremely vigilant. One or two walruses will be on patrol as guardians, and as soon as any unforeseen circumstances are discovered, warning signals will be launched. The following is a definition of the danger and safety signals in WO.

The pseudo code and flowchart of WO are described in detail in Algorithm 1 and Figure 2, respectively.

Algorithm 1. This is the WO algorithm pseudocode.

1) Adjust the population and describe the related variables.
2) Estimate the fitness function and extract the best solutions.
3) While $t < T$
4) If $|Danger\ signal\ > 1|$
5) Update each walrus position using Eq (22)
6) Else
7) If $Safety\ signal\ \geq\ 0.5$
8) For walrus is male
9) Apply Halton sequence to update new position.
10) For walrus is female
11) Apply Eq (25) to update new position.
12) For walrus is juvenile
13) Apply Eq (26) to update new position.
14) End

15) Else If $|Danger\ signal| \geq 0.5$
16) Apply Eq. (30) to update new position.
17) Else
18) Apply Eq. (31) to update new position.
19) End
20) Update the position of walrus.
21) Calculate the fitness function and extract the best solutions.
22) t = t + 1
23) End

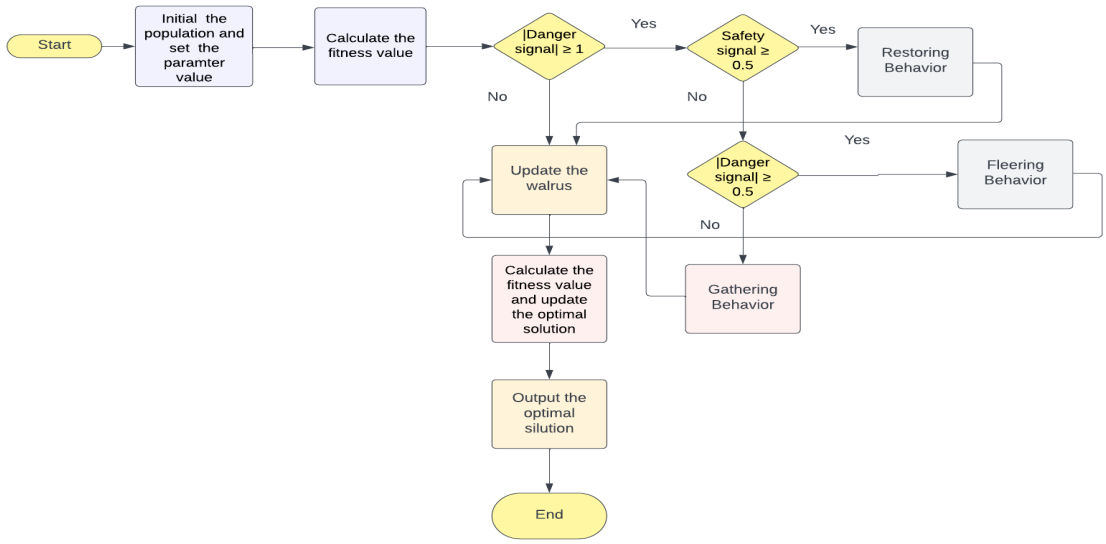

Figure 2. Flow chart of WO algorithm [54].

5. Results

5.1. Analysis of results for PEMFC

The optimal variables of a Ned stack PS6 have been defined by using the WO algorithm. The proposed WO method is compared with other techniques such as the Tunicate Swarm Algorithm (TSA) [55], the Harris Hawks Optimizer (HHO) [56], the Heap Based Optimizer (HBO) [57], the Chimp Optimization Algorithm (ChOA) [58], and the Osprey Optimization Algorithm (OOA) [59]. Experimental data of Ned stack PS6 have been applied to measure the reliability and accuracy of all algorithms. The identified variables at the best SSE for PEMFC are illustrated in Table 2. Based on Table 2, the best SSE is achieved by the WO algorithm with the value 1.945415603, then HBO, HHO, TSA, ChOA, and OOA, respectively. The estimated parameters for each algorithm over 30 runs are described in Tables 3–8 for WO, OOA, TSA, ChOA, HHO, and HBO, respectively. The identified value of voltage for all techniques at the best run is reported in Table 9 compared to the measured value.

Each algorithm is evaluated once it has been run thirty times on its own. Accuracy and reliability are the metrics used to evaluate each algorithm. The standard deviation of the SSE value and the lowest SSE value associated with the accuracy of the algorithm are indicated for every method that is

described in terms of reliability. Table 10 provides more clarity on the statistical analysis of PEMFC for all running algorithms. Based on these data, the recommended WO method achieves the highest accuracy, followed by HHO, HBO, TSA, ChOA, and OOA.

The convergence of the iteration in each run is the primary criteria used to categorize the performance of the algorithms, and the behavior of each algorithm is compared with the robustness data of each of the thirty distinct runs. The robustness and convergence of each PEMFC algorithm are shown in Figures 3 and 4, respectively. These figures demonstrate the great degree of resilience, dependability, and convergence of quicker performance of the proposed WO method.

Table 2. The parameters identified for PEMFC at the best SSE.

Method	WO	**OOA**	**TSA**	**ChOA**	**HHO**	**HBO**
$\boldsymbol{\delta_1}$	−0.853200569	−0.959544011	−1.19978	−1.19978	−0.8532	−1.070939173
$\boldsymbol{\delta_2}$	0.002354536	0.003156872	0.003915906	0.003378166	0.002353465	0.002997364
$\boldsymbol{\delta_3}$	0.000034100	0.000067400	0.0000717	0.0000340	0.0000340	0.00003400
$\boldsymbol{\delta_4}$	−0.000095400	−0.000099700	−0.0000954	−0.0000954	−0.0000954	−0.00009540
$\boldsymbol{\gamma}$	13	16.4290859	13	13	13	13
B	0.001879210	0.040533253	0.001726088	0.002323305	0.001895643	0.001881396

Table 3. Decision variables based on WO method over 30 independent runs.

$\boldsymbol{\delta_1}$	$\boldsymbol{\delta_2}$	$\boldsymbol{\delta_3}$	$\boldsymbol{\delta_4}$	$\boldsymbol{\gamma}$	**B**
−0.853566554	0.002465614	0.0000418	−0.0000954	13	0.001875769
−0.860055821	0.002409862	0.0000365	−0.0000954	13	0.001877519
−0.854034366	0.002465031	0.0000417	−0.0000954	13.35302298	0.007404403
−0.853244703	0.002475315	0.0000425	−0.0000954	13.04761331	0.002715849
−0.878601137	0.002517158	0.0000403	−0.0000954	14.90291269	0.02757478
−0.853352949	0.002438533	0.0000400	−0.0000954	14.07170862	0.017467133
−1.00879319	0.00281544	0.0000341	−0.0000954	13	0.001879238
−0.914605236	0.002559889	0.0000358	−0.0000954	13.6461961	0.011697043
−0.853210792	0.002640961	0.0000542	−0.0000954	14.25241647	0.019757951
−0.856139511	0.002426655	0.0000385	−0.0000954	13.29215144	0.006492031
−0.951294729	0.002772022	0.0000430	−0.0000954	13.00018172	0.001907953
−0.853202153	0.002452071	0.0000409	−0.0000954	13	0.001875291
−0.911720781	0.00277847	0.0000517	−0.0000954	13.15255592	0.004358724
−0.853216948	0.002369916	0.0000352	−0.0000954	13.40237971	0.008111968
−0.855282035	0.00235925	0.0000340	−0.0000954	13.67445541	0.012109187
−0.853251916	0.00237229	0.0000353	−0.0000954	13.06371306	0.002942062
−0.890303859	0.002486264	0.0000356	−0.0000954	13	0.001877507
−0.853207846	0.002492915	0.0000438	−0.0000954	13.83465142	0.014295513
−0.907495971	0.002945623	0.0000645	−0.0000954	17.73888927	0.053307413
−0.853200569	0.002354536	0.0000341	−0.0000954	13	0.00187921
−1.076368584	0.003028541	0.0000355	−0.0000954	21.88758647	0.076779435
−0.853313815	0.002459558	0.0000414	−0.0000954	13.08302722	0.00324834

Continued on next page

δ_1	δ_2	δ_3	δ_4	γ	B
−0.8532	0.002367934	0.0000350	−0.0000954	13	0.001878355
−0.85320016	0.002612978	0.0000522	−0.0000954	13.32724572	0.007028232
−1.043821036	0.002922534	0.0000344	−0.0000954	13	0.001878723
−0.989700863	0.00289034	0.0000433	−0.0000954	13	0.001872944
−0.866615934	0.002718634	0.0000569	−0.0000954	13.45797988	0.008943924
−0.853690792	0.002399199	0.0000371	−0.0000954	13	0.001877249
−0.859230426	0.002481247	0.0000418	−0.0000954	15.34033061	0.032242822
−0.882443934	0.00243979	0.0000340	−0.0000954	13.35344806	0.007430101

Table 4. Decision variables based on OOA method over 30 independent runs.

δ_1	δ_2	δ_3	δ_4	γ	B
−0.876868537	0.002493939	0.0000356	−0.000106684	13.74027463	0.012771761
−0.887931097	0.002639118	0.0000421	−0.000106279	14.38230501	0.037357767
−0.853410829	0.002484147	0.0000385	−0.000104000	14.93221095	0.057048747
−0.931995177	0.002718515	0.0000392	−0.000107726	14.29361053	0.024945846
−1.100061194	0.003260373	0.0000424	−0.000104569	15.63284192	0.0489365
−1.000440472	0.003099187	0.0000518	−0.0000996	15.48566937	0.060832688
−1.022011441	0.003453348	0.0000678	−0.000123604	16.56981686	0.044582211
−0.854635589	0.002464316	0.0000353	−0.000112881	15.21003277	0.041000782
−0.911314079	0.002800247	0.0000483	−0.000107	14.56339828	0.039082666
−0.890187675	0.002821552	0.0000535	−0.000105545	15.42780591	0.059397543
−0.888751818	0.002775527	0.0000486	−0.000117576	15.54415574	0.044937602
−0.8532	0.002781281	0.0000509	−0.000142982	15.97168209	0.040706577
−0.8532	0.002770209	0.0000568	−0.000118277	16.29152661	0.040778951
−0.876764731	0.002710289	0.0000491	−0.000106873	15.43076484	0.049481236
−0.8532	0.002732368	0.0000534	−0.000119425	15.0627159	0.034286176
−0.886317363	0.00271603	0.0000484	−0.00010398	15.20572317	0.045709089
−0.860594658	0.002556515	0.0000440	−0.000100955	14.4467673	0.033637808
−0.919600216	0.002864965	0.0000531	−0.000103218	16.46197817	0.049430129
−0.8532	0.002782358	0.0000607	−0.000114	14.95320092	0.012091416
−0.882103162	0.002670587	0.0000473	−0.000100466	14.86506182	0.041740177
−0.8532	0.002900991	0.0000690	−0.000106347	15.65852255	0.038243091
−0.881280378	0.002763002	0.0000507	−0.000106617	15.33934736	0.060479061
−0.8568493	0.002491801	0.0000357	−0.000116573	14.45140644	0.033262212
−0.8532	0.002720026	0.0000546	−0.000118757	15.49541598	0.020134576
−0.920261639	0.003034928	0.0000643	−0.000105418	14.4716418	0.029886722
−0.853349402	0.00289854	0.0000664	−0.000115299	17.3251641	0.056397862
−0.87241851	0.002643922	0.0000424	−0.000116	15.01868166	0.046869631
−0.8532	0.003087222	0.0000781	−0.000130457	17.95015698	0.042465833
−0.959544011	0.003156872	0.0000674	−0.0000997	16.4290859	0.040533253
−0.8532	0.002600618	0.0000412	−0.000135935	16.01642909	0.025500384

Table 5. Decision variables based on TSA method over 30 independent runs.

δ_1	δ_2	δ_3	δ_4	γ	B
−0.8532	0.002839092	0.0000681	−0.0000954	14.91980312	0.029388202
−1.142296738	0.003215667	0.0000348	−0.0000954	17.17361894	0.048467835
−1.19978	0.00403395	0.0000807	−0.0000954	22.15688282	0.076245532
−1.108021609	0.003914985	0.0000909	−0.0000954	13.41737676	0.007438607
−1.153828831	0.003474449	0.0000505	−0.0000954	14.38133988	0.020308248
−0.855646951	0.002447642	0.0000403	−0.0000954	13	0
−0.87493782	0.002871171	0.0000661	−0.0000954	17.41755797	0.050509
−1.061939659	0.003882615	0.0000980	−0.0000954	13.50364601	0.009268655
−1.114356868	0.004036595	0.0000980	−0.0000954	17.52147507	0.052757555
−1.019017486	0.003013811	0.0000462	−0.0000954	20.24849866	0.068429609
−1.19978	0.003915906	0.0000717	−0.0000954	13	0.001726088
−1.118857297	0.003331782	0.0000476	−0.0000954	16.01563608	0.0395123
−0.934872392	0.003503072	0.0000980	−0.0000954	18.80475917	0.060819979
−0.867129294	0.003198632	0.0000905	−0.0000954	15.97861925	0.039666553
−1.040580141	0.003819591	0.0000980	−0.0000954	13.77398628	0.013174976
−1.11635963	0.003461507	0.0000575	−0.0000954	22.45766349	0.079334084
−1.19978	0.003466757	0.0000404	−0.0000954	16.37706932	0.041086981
−1.138949003	0.003221227	0.0000357	−0.0000954	16.67579986	0.045452198
−1.008924887	0.002897987	0.0000400	−0.0000954	15.66553156	0.034779811
−0.916855394	0.002537812	0.0000340	−0.0000954	17.77717367	0.053749874
−1.062643103	0.003159506	0.0000470	−0.0000954	13.44544609	0.009590924
−0.906778667	0.003058066	0.0000724	−0.0000954	13.43040137	0.008133108
−0.859437007	0.002862126	0.0000687	−0.0000954	17.64720308	0.052016151
−1.19978	0.004193075	0.0000911	−0.0000954	15.02724831	0.030428843
−1.19978	0.004029188	0.0000800	−0.0000954	16.91836486	0.046340119
−1.017962231	0.003665253	0.0000920	−0.0000954	16.58982553	0.043855626
−1.117924404	0.003496244	0.0000592	−0.0000954	14.97252518	0.02937587
−1.162769702	0.003876079	0.0000766	−0.0000954	13.80542143	0.012966984
−0.8532	0.002507507	0.0000448	−0.0000954	13.86181084	0.014771008
−0.921134326	0.002912696	0.0000593	−0.0000954	14.79524293	0.026513575

Table 6. Decision variables based on ChOA method over 30 independent runs.

δ_1	δ_2	δ_3	δ_4	γ	B
−1.007481827	0.002965622	0.0000449	−0.0000954	13	0
−1.19978	0.003374559	0.0000340	−0.0000954	13	0
−1.19978	0.003479361	0.0000412	−0.0000954	13.03311646	0
−0.948627412	0.002981715	0.0000585	−0.0000954	13	0
−1.19978	0.003375464	0.0000340	−0.0000954	13	0.00000000403
−1.19978	0.003380732	0.0000340	−0.0000954	13	0.002932141
−1.19978	0.003427353	0.0000376	−0.0000954	13	0
−1.19978	0.003373077	0.0000340	−0.0000954	13	0
−0.990867704	0.003195103	0.0000647	−0.0000954	13	0.00000147
−0.878968003	0.002557823	0.0000431	−0.0000954	13	0
−1.19978	0.003375677	0.0000340	−0.0000954	13	0.00000679
−0.8532	0.002519756	0.0000459	−0.0000954	13	0.000132683
−0.8532	0.002350225	0.0000340	−0.0000954	13	0
−1.19978	0.003373885	0.0000340	−0.0000954	13	0.0000000673
−1.102853196	0.003255721	0.0000456	−0.0000954	13	0.00000163
−1.166241947	0.003831538	0.0000730	−0.0000954	13	0
−1.19978	0.003630332	0.0000519	−0.0000954	13	0.00000354
−1.132352423	0.004023098	0.0000934	−0.0000954	13	0
−1.19978	0.003378166	0.0000340	−0.0000954	13	0.002323305
−1.19978	0.003553335	0.0000465	−0.0000954	13	0
−0.971360092	0.002769616	0.0000389	−0.0000954	13	0
−1.19978	0.003375375	0.0000340	−0.0000954	13	0
−1.19978	0.003375794	0.0000340	−0.0000954	13	0
−0.888689573	0.002608552	0.0000448	−0.0000954	13	0
−0.8532	0.002349652	0.0000340	−0.0000954	13	0
−0.8532	0.00235057	0.0000340	−0.0000954	13	0
−1.19978	0.00337634	0.0000340	−0.0000954	13	0
−1.19978	0.003376093	0.0000340	−0.0000954	13	0
−1.19978	0.003952869	0.0000744	−0.0000954	13	0
−1.19978	0.003377145	0.0000340	−0.0000954	13	0

Table 7. Decision variables based on HHO method over 30 independent runs.

δ_1	δ_2	δ_3	δ_4	γ	B
−0.8532	0.002508947	0.0000449	−0.0000954	14.47508168	0.022847632
−0.8532	0.00278092	0.0000643	−0.0000954	18.77462834	0.059957609
−0.853938468	0.003127229	0.0000886	−0.0000954	21.15061860	0.072837725
−0.8532	0.00306406	0.0000839	−0.0000954	13.12590230	0.003933532
−0.8532	0.002448545	0.0000408	−0.0000954	14.61429442	0.024135781
−1.065675163	0.003373452	0.0000554	−0.0001177	19.37768932	0.061682283
−0.877225152	0.002586985	0.0000442	−0.0000982	13.90782264	0.018923601
−0.853346084	0.002383782	0.0000360	−0.0000954	13.68772648	0.013348001
−0.8535834	0.002825701	0.0000676	−0.0000954	21.99718801	0.076501157
−0.853216313	0.002408132	0.0000379	−0.0000954	14.51426962	0.02307025
−0.8532	0.002545598	0.0000475	−0.0000954	13.09983751	0.003558152
−0.8532	0.002394252	0.0000369	−0.0000954	14.18108526	0.018822875
−0.853375743	0.002480956	0.0000429	−0.0000954	13.87342476	0.015300754
−0.8532	0.002353465	0.0000340	−0.0000954	13	0.001895643
−0.871448882	0.002731344	0.0000566	−0.0000960	14.8270774	0.02679571
−0.853212556	0.002717227	0.0000597	−0.0000954	15.76810724	0.03666253
−0.854705556	0.00235916	0.0000345	−0.0000956	20.39640625	0.069164604
−0.8532	0.002837859	0.0000681	−0.0000954	15.51125522	0.03385145
−0.8532	0.002353139	0.0000342	−0.0000954	16.87360931	0.046475373
−0.853208767	0.002416617	0.0000382	−0.0000954	13.74456471	0.014972333
−0.8532	0.002374141	0.0000355	−0.0000954	13.84858962	0.014490863
-0.8532	0.002606228	0.0000518	−0.0000954	13.39950293	0.007911236
−0.8532	0.003257447	0.0000976	−0.0000954	13	6.06E-06
−0.85443684	0.002590895	0.0000505	−0.0000955	15.83576209	0.037406685
−0.8532	0.002454603	0.0000412	−0.0000954	14.15302645	0.018362267
−0.867922123	0.00259887	0.0000475	−0.0000971	13.68935123	0.013892949
−0.8532	0.002440901	0.0000402	−0.0000954	14.60973316	0.024115853
−0.853206657	0.002785937	0.0000645	−0.0000954	15.43650016	0.033096236
−0.853238223	0.002535794	0.0000470	−0.0000954	16.99515789	0.047126659
−0.8532	0.002354485	0.0000343	−0.0000954	13.05041363	0.001129183

Table 8. Decision variables based on HBO method over 30 independent runs.

δ_1	δ_2	δ_3	δ_4	γ	B
−1.19978	0.003375064	0.0000340	−0.0000954	15.93435562	0.037623165
−0.8532	0.003161331	0.0000907	−0.0000954	13	0.001637862
−0.8532	0.002414839	0.0000383	−0.0000954	13	0.001872528
−0.982774043	0.003137423	0.0000623	−0.0000954	16.12247875	0.039307531
−1.079699185	0.003018536	0.0000340	−0.0000954	18.13106837	0.055738717
−0.8532	0.00262885	0.0000535	−0.0000954	16.87587354	0.046953428
−1.16227075	0.003271385	0.0000344	−0.0000954	15.84740104	0.037386249
−0.8532	0.002525645	0.0000462	−0.0000954	15.27110773	0.031584571
−0.8532	0.002639363	0.0000543	−0.0000954	16.87332069	0.046676856
−1.186418894	0.003338544	0.0000340	−0.0000954	13.00679931	0.001734876
−0.882468653	0.003301148	0.0000944	−0.0000954	13	0.001938518
−0.8532	0.002870705	0.0000703	−0.0000954	13	0.001499429
−0.999643544	0.00296983	0.0000471	−0.0000954	17.54762778	0.051851765
−1.141584692	0.003706593	0.0000691	−0.0000954	13	0.001876189
−0.988514778	0.003130083	0.0000604	−0.0000954	13	0.001933796
−0.853200302	0.003245938	0.0000966	−0.0000954	13	0.001844955
−1.199759839	0.004208753	0.0000922	−0.0000954	13	0.002104947
−1.01845926	0.003550067	0.0000836	−0.0000954	13	0.002490088
−1.034332177	0.002995397	0.0000419	−0.0000954	21.46469936	0.074837822
−1.027835087	0.003625759	0.0000872	−0.0000954	15.69722095	0.03494139
−1.19978	0.003987285	0.0000768	−0.0000954	14.27889223	0.020135876
−1.124194548	0.004067427	0.0000980	−0.0000954	13	0.002056482
−1.024568268	0.003156432	0.0000548	−0.0000954	13	0.002105551
−1.070939173	0.002997364	0.0000340	−0.0000954	13	0.001881396
−1.036228901	0.0029231	0.0000361	−0.0000954	13	0.000607177
−0.983783132	0.003627683	0.0000963	−0.0000954	13	0.001850845
−1.159143642	0.003490548	0.0000507	−0.0000954	22.12136763	0.077864772
−0.866706674	0.002544769	0.0000446	−0.0000954	13.05077882	0.002535624
−1.004303753	0.002980769	0.0000466	−0.0000954	13	0.002227467
−0.939330766	0.003222175	0.0000771	−0.0000954	13	0.002001052

Table 9. Comparison between estimated and measured voltage at the best solution.

Measured	WO	OOA	TSA	ChOA	HHO	HBO
[60]	Estimated					
61.64	62.29744305	62.50342539	62.28630234	62.29273736	62.29798587	62.29770348
59.57	59.75409932	59.86080435	59.74308000	59.74893550	59.75462526	59.75435757
58.94	59.03019752	59.11231350	59.01923984	59.02480188	59.03071491	59.03045466
57.54	57.49139398	57.52896066	57.48062516	57.48529148	57.49188532	57.49164775
56.8	56.71799092	56.73768097	56.70735138	56.71140739	56.71846454	56.71824240
56.13	56.04843580	56.05523751	56.03792836	56.04136307	56.04889138	56.04868494
55.23	55.16506537	55.15852770	55.15476155	55.15724294	55.16549332	55.16531093
54.66	54.63017328	54.61752516	54.62000903	54.6218400	54.63058240	54.63041640
53.61	53.64473773	53.62448041	53.63486224	53.63535481	53.64510816	53.64497583
52.86	52.95647330	52.93349248	52.94682328	52.9462773	52.95681374	52.95670751
51.91	51.45212335	51.42959800	51.44303190	51.43993605	51.45239036	51.45234802
51.22	51.03934667	51.01827089	51.03042383	51.02656424	51.03959172	51.03956848
49.66	49.42878281	49.41757013	49.42057957	49.41348899	49.42893522	49.42899255
49	48.63648708	48.63196910	48.62867362	48.61985055	48.63658995	48.63669035
48.15	48.03952436	48.04055011	48.03202028	48.02183023	48.03958820	48.03972254
47.52	47.64434634	47.64918624	47.63705456	47.62593039	47.64438354	47.64454104
47.1	47.05473122	47.06534710	47.04776745	47.03520596	47.05472748	47.05492057
46.48	46.25839538	46.27667866	46.25189652	46.23730955	46.25833404	46.25857720
45.66	45.45459558	45.48000049	45.44859239	45.43185996	45.45447333	45.45476942
44.85	44.84079504	44.87087076	44.83518901	44.8167472	44.84062435	44.84096253
44.24	44.01793820	44.05269188	44.01289131	43.99205647	44.01769978	44.01809681
42.45	42.97417032	43.01111406	42.96987987	42.94583059	42.97384113	42.97431701
41.66	42.11693282	42.15133341	42.11330674	42.08645402	42.11652462	42.11706913
40.68	41.01379005	41.03702440	41.01108293	40.98037953	41.01327354	41.01391211
40.09	40.34402671	40.35490906	40.34191684	40.30872599	40.34344036	40.34413957
39.51	39.65120245	39.64376812	39.6497455	39.61384773	39.65054021	39.65130532
38.73	38.71236587	38.66906359	38.71185798	38.67204638	38.71159406	38.71245429
38.15	37.99603248	37.91483588	37.99630568	37.95328958	37.99517110	37.99610907
37.38	37.00844756	36.85607400	37.00989327	36.96209183	37.00745263	37.00850651

Table 10. Statistical analysis for PEMFC.

	Min	**SD**	**Mean**	**Max**
WO	1.945415603	0.124810273	1.997965615	2.574660996
OOA	2.592017414	11.11761897	17.63689506	54.21971512
TSA	1.947319234	0.175716922	2.165255368	2.642701240
ChOA	1.961109131	0.034884510	2.04	2.134193004
HHO	1.945421572	1.647991725	2.445014898	11.07849906
HBO	1.945416441	0.174253930	2.059032058	2.594772932

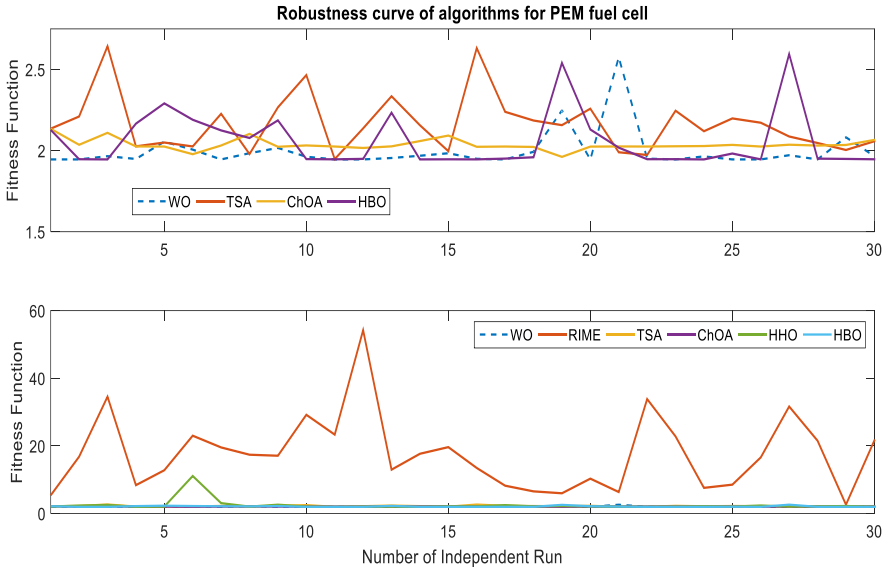

Figure 3. Robustness curves for all algorithms.

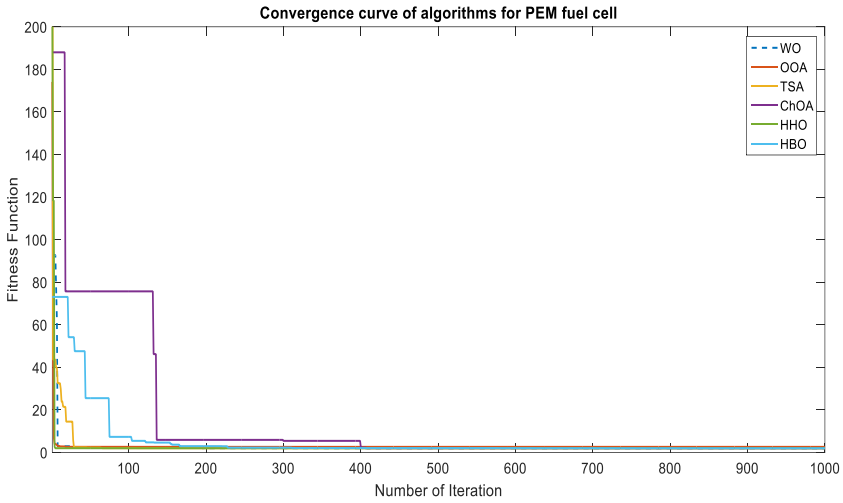

Figure 4. Convergence curves for all algorithms.

5.2. Discussion

The optimal variables of a Ned stack PS6 have been identified by using the WO algorithm. The proposed WO method is compared with other techniques such as TSA, HHO, the HBO, ChOA, and OOA. These methods are applied for the same problem at the same environmental conditions. Also, the proposed WO method is compared with methods of other published works such as the Equilibrium Optimizer (EO), manta rays foraging optimizer (MRFO), neural network algorithm (NNA), artificial ecosystem optimizer (AEO), slap swarm optimizer (SSO), and vortex search approach with DE (VSDE). Table 11 explains the comparative analysis between all algorithms. Based on the data in Table 11, the proposed WO technique achieves the best SSE for PEMFC. The relation between the estimated

voltage from the WO method and the measured voltage is described in Figure 5. Also, this figure contains the absolute error for the voltage. These figures demonstrate the great degree of closeness of the identified results from the proposed WO method and the measured results.

Table 11. Comparison of the best fitness function of WO with other algorithms for PEMFC.

	Min
WO	1.945415603
OOA	2.592017414
TSA	1.947319234
ChOA	1.961109131
HHO	1.945421572
HBO	1.945416441
EO [60]	1.9547
MRFO [60]	2.1360
NNA [60]	2.1449
AEO [60]	2.1459
SSO [60]	2.1807
VSDE [60]	2.0885
ISA [60]	1.9564
ABC [60]	1.9663
BSA [60]	1.9664

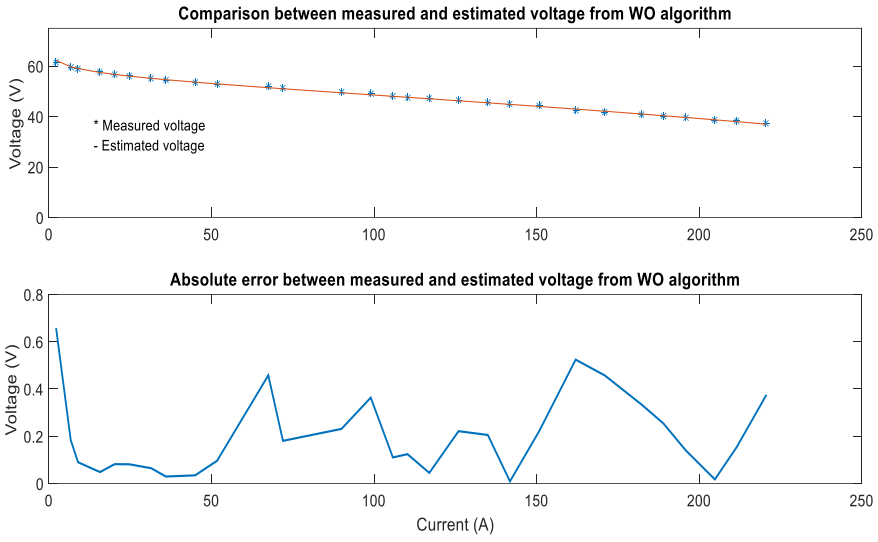

Figure 5. Comparison between identified and measured voltage for PEMFC based on WO method.

6. Conclusions

The ideal parameter identification procedure for the Ned Stack PS6 PEM fuel-cell model has been investigated in this research work using a number of recent optimization approaches. The six optimization strategies listed below have been examined: the Walrus Optimizer, the Osprey

Optimization Algorithm, the Tunicate Swarm Algorithm, the Harris Hawks Optimization, the Heap Based Optimizer, and the Chimp Optimization Algorithm. Also, the proposed Walrus Optimizer method is compared with methods in other published works such as the Equilibrium Optimizer, Manta rays Foraging Optimizer, Neural Network Algorithm, Artificial Ecosystem Optimizer, Slap Swarm Optimizer, and Vortex Search with DE. The sum square error between the estimated and measured cell voltages is the fitness function that must be minimized, and these six parameters act as choice variables during optimization. It was discovered that the ideal fitness function fell between 1.945415603 and 2.779793414. OOA produced the greatest value, 2.779793414, while the WO method produced the lowest result, 1.945415603. The standard deviation ranged from 11.11761897 to 0.124810273. With a standard deviation of 0.124810273, WO had the lowest value, and OOA had the highest value, 11.11761897. Using the SSE as the objective function allows the WO to anticipate outcomes more accurately, according to the data gathered. It also ensures faster convergence than other metaheuristic algorithms studied, which makes it a feasible solution for global optimization problems outside of fuel cell-related ones. Also, the great degree of closeness of the identified results from the proposed WO method and the measured results is clarified according to the results. Future large-scale, practical optimization issues involving power systems and solar energy will be resolved using the WO technique. This work was limited to parameter identification for the Ned Stack PS6 PEM fuel-cell model, which restricts its applicability to other fuel cell models or uses. The future effort involves expanding the study to include various fuel cell models or applications to evaluate the effectiveness and reliability of the Walrus Optimizer technique in diverse fields.

Use of AI tools declaration

The authors declare they have not used Artificial Intelligence (AI) tools in the creation of this article.

Funding

This research was funded by Princess Nourah bint Abdulrahman University Researchers Supporting Project number (PNURSP2024R407), Princess Nourah bint Abdulrahman University, Riyadh, Saudi Arabia.

Acknowledgments

The authors would like to express their thanks to Princess Nourah bint Abdulrahman University Researchers Supporting Project number (PNURSP2024R407), Princess Nourah bint Abdulrahman University, Riyadh, Saudi Arabia.

Conflict of interest

The authors declare there is no conflict of interest.

References

1. M. N. Ali, K. Mahmoud, M. Lehtonen, M. M. F. Darwish, Promising MPPT methods combining metaheuristic, fuzzy-logic and ANN techniques for grid-connected photovoltaic, *Sensors*, **21** (2021), 1244. https://doi.org/10.3390/s21041244
2. D. S. AbdElminaam, E. H. Houssein, M. Said, D. Oliva, A. Nabil, An efficient heap-based optimizer for parameters identification of modified photovoltaic models, *Ain Shams Eng. J.*, **13** (2022), 101728. https://doi.org/10.1016/j.asej.2022.101728
3. A. A. K. Ismaeel, E. H. Houssein, D. Oliva, M. Said, Gradient-based optimizer for parameter extraction in photovoltaic models, *IEEE Access*, **9** (2021), 13403–13416. https://doi.org/10.1109/ACCESS.2021.3052153
4. E. H. Houssein, S. Deb, D. Oliva, H. Rezk, H. Alhumade, M. Said, Performance of gradient-based optimizer on charging station placement problem, *Mathematics*, **9** (2021), 2821. https://doi.org/10.3390/math9212821
5. D. S. Abdelminaam, M. Said, E. H. Houssein, Turbulent flow of water-based optimization using new objective function for parameter extraction of six photovoltaic models., *IEEE Access*, **9** (2021), 35382–35398. https://doi.org/10.1109/ACCESS.2021.3061529
6. M. Said, E. H. Houssein, S. Deb, A. A. Alhussan, R. M. Ghoniem, A novel gradient-based optimizer for solving unit commitment problem, *IEEE Acces*s, **10** (2022), 18081–18092. https://doi.org/10.1109/ACCESS.2022.3150857
7. E. H. Houssein, D. Oliva, N. A. Samee, N. F. Mahmoud, M. M. Emam, Liver cancer algorithm: A novel bio-inspired optimizer, *Comput. Biol. Med.*, **165** (2023), 107389. https://doi.org/10.1016/j.compbiomed.2023.107389
8. S. Li, H. Chen, M. Wang, A. A. Heidari, S. Mirjalili, Slime mould algorithm: A new method for stochastic optimization, *Future Gener. Comp. Syst.*, **111** (2020), 300–323. https://doi.org/10.1016/j.future.2020.03.055
9. Y. Yang, H. Chena, A. A. Heidari, A. H. Gandomi, Hunger games search: Visions, conception, implementation, deep analysis, perspectives, and towards performance shifts, *Expert Syst. Appl.*, **177** (2021), 114864. https://doi.org/10.1016/j.eswa.2021.114864
10. I. Ahmadianfar, A. A. Heidari, A. H. Gandomi, X. Chu, H. Chen, RUN beyond the metaphor: An efficient optimization algorithm based on Runge Kutta method, *Expert Syst. Appl.*, **181** (2021), 115079. https://doi.org/10.1016/j.eswa.2021.115079
11. I. Ahmadianfar, A. A. Heidari, S. Noshadian, H. Chen, A. H. Gandomi, INFO: An efficient optimization algorithm based on weighted mean of vectors, *Expert Syst. Appl.*, **195** (2022), 116516. https://doi.org/10.1016/j.eswa.2022.116516
12. X. Yuan, Y. Liu, R. Bucknall, A novel design of a solid oxide fuel cell-based combined cooling, heat and power residential system in the U. K., *IEEE T. Ind. Appl.*, **57** (2021), 805–813. https://doi.org/10.1109/TIA.2020.3034073
13. J. Ihonen, P. Koski, V. Pulkkinen, T. Keränen, H. Karimäki, S. Auvinen, et al., Operational experiences of PEMFC pilot plant using low grade hydrogen from sodium chlorate production process. *Int. J. Hydrogen Energ.*, **42** (2017), 27269–27283. https://doi.org/10.1016/j.ijhydene.2017.09.056

14. Y. Qiu, P. Wu, T. Miao, J. Liang, K. Jiao, T. Li, et al., An intelligent approach for contact pressure optimization of PEM fuel cell gas diffusion layers, *Appl. Sci.*, **10** (2020), 4194. https://doi.org/10.3390/app10124194
15. K. Ahmed, O. Farrok, M. M. Rahman, M. S. Ali, M. M. Haque, A. K. Azad, Proton exchange membrane hydrogen fuel cell as the grid connected power generator, *Energies*, **13** (2020), 6679. https://doi.org/10.3390/en13246679
16. K. Nikiforow, J. Pennanen, J. Ihonen, S. Uski, P. Koski, Power ramp rate capabilities of a 5 kW proton exchange membrane fuel cell system with discrete ejector control. *J. Power Sources*, **381** (2018), 30–37. https://doi.org/10.1016/j.jpowsour.2018.01.090
17. A. S. Menesy, H. M. Sultan, A. Korashy, F. A. Banakhr, M. G. Ashmawy, S. Kamel, Effective parameter extraction of different polymer electrolyte membrane fuel cell stack models using a modified artificial ecosystem optimization algorithm, *IEEE Access*, **8** (2020), 31892–31909. https://doi.org/10.1109/ACCESS.2020.2973351
18. B. Sundén, Fuel cell types—Overview. In: *Hydrogen, batteries and fuel cells*, Cambridge, MA, USA: Academic Press, 2019, 123–144. https://doi.org/10.1016/B978-0-12-816950-6.00008-7
19. A. Fathy, H. Rezk, Multi-verse optimizer for identifying the optimal parameters of PEMFC model, *Energy*, **143** (2018), 634–644. https://doi.org/10.1016/j.energy.2017.11.014
20. H. Ashraf, S. O. Abdellatif, M. M. Elkholy, A. A. El-Fergany, Computational techniques based on artificial intelligence for extracting optimal parameters of PEMFCs: Survey and insights, *Arch. Comput. Methods Eng.*, **29** (2022), 3943–3972. https://doi.org/10.1007/s11831-022-09721-y
21. H. Rezk, A. G. Olabi, E. Sayed, T. Wilberforce, Role of metaheuristics in optimizing microgrids operating and management issues: A comprehensive review, *Sustainability*, **15** (2023), 4982. https://doi.org/10.3390/su15064982
22. Y. Zhu, N. Yousefi, Optimal parameter identification of PEMFC stacks using adaptive sparrow search algorithm, *Int. J. Hydrogen Energ.*, **46** (2021), 9541–9552. https://doi.org/10.1016/j.ijhydene.2020.12.107
23. D. Yousri, S. Mirjalili, J. A. T. Machado, S. B. Thanikanti, O. Elbaksawi, A. Fathy, Efficient fractional-order modified Harris hawks optimizer for proton exchange membrane fuel cell modeling, *Eng. Appl. Artif. Intel.*, **100** (2021), 104193. https://doi.org/10.1016/j.engappai.2021.104193
24. Z. Yuan, W. Wang, H. Wang, A. Yildizbasi, Developed coyote optimization algorithm and its application to optimal parameters estimation of PEMFC model, *Energy Rep.*, **6** (2020), 1106–1117. https://doi.org/10.1016/j.egyr.2020.04.032
25. S. Bao, A. Ebadi, M. Toughani, J. Dalle, A. Maseleno, Baharuddin, et al., A new method for optimal parameters identification of a PEMFC using an improved version of monarch butterfly optimization algorithm, I*nt. J. Hydrogen Energ.*, **45** (2020), 17882–17892. https://doi.org/10.1016/j.ijhydene.2020.04.256
26. T. Wilberforce, H. Rezk, A. G. Olabi, E. I. Epelle, M. A. Abdelkareem, Comparative analysis on parametric estimation of a PEM fuel cell using metaheuristics algorithms, *Energy*, **262** (2023), 125530. https://doi.org/10.1016/j.energy.2022.125530
27. A. Fathy, M. A. Elaziz, A. G. Alharbi, A novel approach based on hybrid vortex search algorithm and differential evolution for identifying the optimal parameters of PEM fuel cell, *Renew. Energ.*, **146** (2020), 1833–1845. https://doi.org/10.1016/j.renene.2019.08.046

28. Z. Yuan, W. Wang, H. Wang, Optimal parameter estimation for PEMFC using modified monarch butterfly optimization, *Int. J. Energ. Res.*, **44** (2020), 8427–8441. https://doi.org/10.1002/er.5527
29. Z. Yuan, W. Wang, H. Wang, N. Razmjooy, A new technique for optimal estimation of the circuit-based PEMFCs using developed Sunflower Optimization Algorithm, *Energy Rep.*, **6** (2020), 662–671. https://doi.org/10.1016/j.egyr.2020.03.010
30. S. Sun, Y. Su, C. Yin, K. Jermsittiparsert, Optimal parameters estimation of PEMFCs model using converged moth search algorithm, *Energy Rep.*, **6** (2020), 1501–1509. https://doi.org/10.1016/j.egyr.2020.06.002
31. R. Syah, L. A. Isola, J. W. G. Guerrero, W. Suksatan, D. Sunarsi, M. Elveny, et al., Optimal parameters estimation of the PEMFC using a balanced version of Water Strider Algorithm, *Energy Rep.*, **7** (2021), 6876–6886. https://doi.org/10.1016/j.egyr.2021.10.057
32. H. Guo, H. Tao, S. Q. Salih, Z. M. Yaseen, Optimized parameter estimation of a PEMFC model based on improved Grass Fibrous Root Optimization Algorithm, *Energy Rep.*, **6** (2020), 1510–1519. https://doi.org/10.1016/j.egyr.2020.06.001
33. M. A. Mossa, O. M. Kamel, H. M. Sultan, A. A. Z. Diab, Parameter estimation of PEMFC model based on Harris Hawks' optimization and atom search optimization algorithms, *Neural Comput. Appl.*, **33** (2021), 5555–5570. https://doi.org/10.1007/s00521-020-05333-4
34. H. Rezk, S. Ferahtia, A. Djeroui, A. Chouder, A. Houari, M. Machmoum, et al., Optimal parameter estimation strategy of PEM fuel cell using gradient-based optimizer, *Energy*, **239** (2022), 122096. https://doi.org/10.1016/j.energy.2021.122096
35. G. Zhang, C. Xiao, N. Razmjooy, Optimal parameter extraction of PEM fuel cells by meta-heuristics, *Int. J. Ambient Energy*, **43** (2020), 2510–2519. https://doi.org/10.1080/01430750.2020.1745276
36. W. Han, D. Li, D. Yu, H. Ebrahimian, Optimal parameters of PEM fuel cells using chaotic binary shark smell optimizer, *Energy Sources Part A*, **45** (2019), 7770–7784. https://doi.org/10.1080/15567036.2019.1676845
37. A. Fathy, T. S. Babu, M. A. Abdelkareem, H. Rezk, D. Yousri, Recent approach based heterogeneous comprehensive learning archimedes optimization algorithm for identifying the optimal parameters of different fuel cells, *Energy*, **248** (2022), 123587. https://doi.org/10.1016/j.energy.2022.123587
38. L. Blanco-Cocom, S. Botello-Rionda, L. Ordoñez, S. I. Valdez, Robust parameter estimation of a PEMFC via optimization based on probabilistic model building, *Math. Comput. Simulat.*, **185** (2021), 218–237. https://doi.org/10.1016/j.matcom.2020.12.021
39. X. Lu, D. Kanghong, L. Guo, P. Wang, A. Yildizbasi, Optimal estimation of the proton exchange membrane fuel cell model parameters based on extended version of crow search algorithm, *J. Clean. Prod.*, **272** (2020), 122640. https://doi.org/10.1016/j.jclepro.2020.122640
40. A. S. Menesy, H. M. Sultan, S. Kamel, Extracting model parameters of proton exchange membrane fuel cell using equilibrium optimizer algorithm, In: *2020 International Youth Conference on Radio Electronics, Electrical and Power Engineering (REEPE)*, 2020. https://doi.org/10.1109/REEPE49198.2020.9059219
41. B. Duan, Q. Cao, N. Afshar, Optimal parameter identification for the proton exchange membrane fuel cell using satin bowerbird optimizer, *Int. J. Energ. Res.*, **43** (2019), 8623–8632. https://doi.org/10.1002/er.4859

42. A. Fathy, S. H. E. A. Aleem, H. Rezk, A novel approach for PEM fuel cell parameter estimation using LSHADE-EpSin optimization algorithm, *Int. J. Energ. Res.*, **45** (2021), 6922–6942. https://doi.org/10.1002/er.6282
43. Z. M. Isa, N. M. Nayan, M. H. Arshad, N. A. M. Kajaan, Optimizing PEMFC model parameters using ant lion optimizer and dragonfly algorithm: A comparative study, *Int. J. Electr. Comput. Eng.*, **9** (2019), 5312–5320. http://dx.doi.org/10.11591/ijece.v9i6.pp5295-5303
44. Y. Song, X. Tan, S. Mizzi, Optimal parameter extraction of the proton exchange membrane fuel cells based on a new Harris Hawks optimization algorithm, *Energy Sources Part A*, 2020, 1–18. https://doi.org/10.1080/15567036.2020.1769230
45. Z. Yang, Q. Liu, L. Zhang, J. Dai, N. Razmjooy, Model parameter estimation of the PEMFCs using improved Barnacles Mating Optimization Algorithm, *Energy*, **212** (2020), 118738. https://doi.org/10.1016/j.energy.2020.118738
46. X. Sun, G. Wang, L. Xu, H. Yuan, N. Yousefi, Optimal estimation of the PEM fuel cells applying deep belief network optimized by improved Archimedes optimization algorithm, *Energy*, **237** (2021), 121532. https://doi.org/10.1016/j.energy.2021.121532
47. H. M. Hasanien, M. A. M. Shaheen, R. A. Turky, M. H. Qais, S. Alghuwainem, S. Kamel, et al., Precise modeling of PEM fuel cell using a novel enhanced transient search optimization algorithm, *Energy*, **247** (2022), 123530. https://doi.org/10.1016/j.energy.2022.123530
48. M. Calasan, S. H. E. A. Aleem, H. M. Hasanien, Z. M. Alaas, Z. M. Ali, An innovative approach for mathematical modeling and parameter estimation of PEM fuel cells based on iterative Lambert W function, *Energy*, **264** (2023), 126165. https://doi.org/10.1016/j.energy.2022.126165
49. T. Wilberforce, A. G. Olabi, H. Rezk, A. Y. Abdelaziz, M. A. Abdelkareem, E. T. Sayed, Boosting the output power of PEM fuel cells by identifying best-operating conditions, *Energ. Convers. Manage.*, **270** (2022), 116205. https://doi.org/10.1016/j.enconman.2022.116205
50. H. Rezk, T. Wilberforce, E. T. Sayed, A. N. M. Alahmadi, A. G. Olabi, Finding best operational conditions of PEM fuel cell using adaptive neuro-fuzzy inference system and metaheuristics, *Energy Rep.*, **8** (2022), 6181–6190. https://doi.org/10.1016/j.egyr.2022.04.061
51. T. Wilberforce, A. G. Olabi, D. Monopoli, M. Dassisti, E. T. Sayed, M. A. Abdelkareem, Design optimization of proton exchange membrane fuel cell bipolar plate, *Energ. Convers. Manage.*, **277** (2023), 116586. https://doi.org/10.1016/j.enconman.2022.116586
52. H. Ashraf, S. O. Abdellatif, M. M. Elkholy, A. A. El-Fergany, Honey badger optimizer for extracting the ungiven parameters of PEMFC model: Steady-state assessment, *Energ. Convers. Manage.*, **258** (2022), 115521. https://doi.org/10.1016/j.enconman.2022.115521
53. S. K. Eelsayed, A. Agwa, E. E. Elattar, A. El-Fergany, Steady-state modelling of pem fuel cells using gradientbased optimizer, *Dyna*, **96** (2021), 520–527. http://doi.org/10.6036/10099
54. M. Han, Z. Du, K. F. Yuen, H. Zhu, Y. Li, Q. Yuan, Walrus optimizer: A novel nature-inspired metaheuristic algorithm, *Expert Syst. Appl.*, **239** (2024), 122413. https://doi.org/10.1016/j.eswa.2023.122413
55. S. Kaur, L. K. Awasthi, A. L. Sangal, G. Dhiman, Tunicate Swarm Algorithm: A new bio-inspired based metaheuristic paradigm for global optimization, *Eng. Appl. Artif. Intel.*, **90** (2020), 103541. https://doi.org/10.1016/j.engappai.2020.103541
56. A. A. Heidari, S. Mirjalili, H. Faris, I. Aljarah, M. Mafarja, H. Chen, Harris hawks optimization: Algorithm and applications, *Future Gener. Comput. Syst.*, **97** (2019), 849–872. https://doi.org/10.1016/j.future.2019.02.028

57. Q. Askari, M. Saeed, I. Younas, Heap-based optimizer inspired by corporate rank hierarchy for global optimization, *Expert Syst. Appl.*, **161** (2020), 113702. https://doi.org/10.1016/j.eswa.2020.113702
58. M. Khishe, M. R. Mosavi, Chimp optimization algorithm, *Expert Syst. Appl.*, **149** (2020), 113338. https://doi.org/10.1016/j.eswa.2020.113338
59. M. Dehghani, P. Trojovský, Osprey optimization algorithm: A new bioinspired metaheuristic algorithm for solving engineering optimization problems, *Front. Mech. Eng.*, **8** (2023), 1126450. https://doi.org/10.3389/fmech.2022.1126450
60. S. I. Seleem, H. M. Hasanie, A. A. El-Fergany, Equilibrium optimizer for parameter extraction of a fuel cell dynamic model, *Renew. Energ.*, **169** (2021), 117–128. https://doi.org/10.1016/j.renene.2020.12.131

AIMS Press